

1,1'-Binaphthyl-based imidazolium chemosensors for highly selective recognition of tryptophan in aqueous solutions†

Li Yang, Song Qin, Xiaoyu Su, Fei Yang, Jingsong You,* Changwei Hu, Rugang Xie and Jingbo Lan*

Received 30th April 2009, Accepted 8th October 2009

First published as an Advance Article on the web 17th November 2009

DOI: 10.1039/b908540h

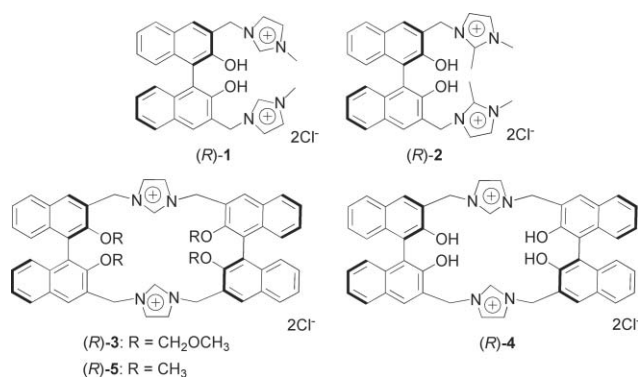
A type of 1,1'-binaphthyl-based imidazolium chemosensor module has been synthesized for the highly selective recognition of tryptophan (Trp) among the eleven α -amino acids investigated in aqueous solutions *via* synergistic effects of multiple hydrogen bonding and electrostatic interactions. These results have demonstrated that the C-2 hydrogen atom of the imidazolium ring plays a key role as a hydrogen bond donor. The UV/vis, fluorescence and mass spectral studies have indicated that a 1 : 1 complex is formed between the host and tryptophan. The binding affinity and selectivity of the cleft-like receptor (*R*)-1 with L-Trp are superior to those of (*R*)-2–5. In spite of an inferior selectivity towards various aromatic amino acids, the macrocyclic (*R*)-3 displays a remarkable enantiodiscrimination for the two enantiomers of tryptophan with a K_D/K_L value as high as 6.2.

Introduction

The development of synthetic receptors capable of recognizing α -amino acids has gained extensive interest in the past few decades because of their biological relevance and practical importance.¹ Despite impressive progress, the design of excellent chemosensors for amino acids in water is still a challenging task in supramolecular chemistry since the formation of hydrogen bonds between guest and receptor molecules is quite difficult in aqueous media.^{2,3} Thus, the vast majority of reported optical detection schemes require prior derivatization of amino acids to amides, alcohols or esters, and proceed in organic solvents.⁴ To overcome the competition from protic solvents for binding sites, positively charged receptors⁵ based on polyammonium,^{5c,6} guanidinium,^{2a,5b,e,7} pyridinium,⁸ polyprotonated azacrown ether,⁹ or metal-containing species^{5a,10} have been developed. Considering the H2 hydrogen at the C2 position of the imidazolium nucleus can serve as a strong hydrogen bond donor due to the relatively high acidity ($pK_a = 21$ – 23),¹¹ the positively charged imidazolium group has been thought of as a new class of promising building blocks to create supramolecular systems. Recently, a variety of receptors bearing imidazolium moieties as binding sites have been designed for anion recognition, mainly various inorganic anions (e.g., F^- , Cl^- , Br^- , I^- , CO_3^{2-} , HCO_3^- , $H_2PO_4^-$, HPO_4^{2-} , PO_4^{3-} , and PF_6^- , etc.), by forming $(C-H)^+ \cdots X^-$ hydrogen bonds between the imidazolium ring and the guest anion.^{5d,12} However, to the best

of our knowledge, molecular recognition of α -amino acids by imidazolium-anchored receptors in aqueous solutions has not yet been reported so far.

The unique chirality and aromatic structure of the 1,1'-binaphthyl scaffold can afford both interesting fluorescence signals and excellent chiral recognition capability. In the last several years, 1,1'-binaphthyls have been well-utilized in designing fluorescence sensors for molecular recognition of organic compounds.^{13,14} In continuation of our ongoing interest in the development of imidazole-based supramolecular chemistry,¹⁵ in this context, we present a strategy for designing the water-soluble 1,1'-bi-2-naphthol (BINOL)-attached chemosensors by incorporating the imidazolium units. The introduction of this kind of positively charged species may not only lead to an improvement of the solubility of receptors in water, but also facilitate enhanced binding affinity and selectivity for guest molecules through multiple hydrogen bonding interactions in an aqueous medium. For this purpose, we herein design a series of cyclic and acyclic imidazolium receptors (*R*)-1–5, and wish to disclose that this class of compounds would serve as significant chemosensors in the fluorescence recognition of tryptophan in aqueous solutions (Scheme 1).



Scheme 1 Imidazolium receptors based on (*R*)-BINOLs.

Key Laboratory of Green Chemistry and Technology of Ministry of Education, College of Chemistry, and State Key Laboratory of Biotherapy, West China Hospital, West China Medical School, Sichuan University, 29 Wangjiang Road, Chengdu, 610064, People's Republic of China. E-mail: jsyu@scu.edu.cn, jingbolan@scu.edu.cn; Fax: +86-28-85412203; Tel: +86-28-85412203

† Electronic supplementary information (ESI) available: Methods and materials of spectra experiments; additional spectroscopic plots and data; the calculation of the association constants, and copies of 1H NMR, ^{13}C NMR and ESI mass spectra; the structures optimized using quantum chemistry. CCDC 729190. For crystallographic data in CIF or other electronic format see DOI: 10.1039/b908540h

Results and discussion

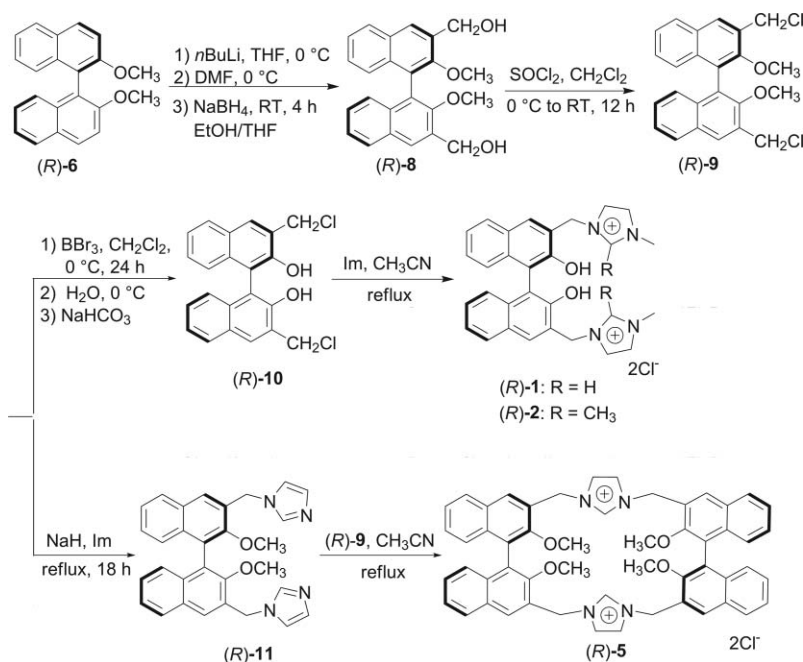
Design and synthesis of binaphthyl-based water-soluble fluorescent sensors (*R*)-1–5

A complex interplay of various factors that control the binding and enantiodiscriminating capability is present in supramolecular systems. Consequently, the rational design of receptors depending on the host's flexibility, cyclic or acyclic form, size, and number of interacting sites may result in enhanced sensitivity and chiral discrimination.¹⁶ In this study, we tried to establish a type of binaphthyl-based imidazolium chemosensor module involving a fluorescent chromophore and a set of stereomatching interaction sites (*e.g.*, hydrogen bond donors and electrostatic interactions). We initially designed the cleft-like receptor (*R*)-1, in which two *N*-methyl imidazolium moieties are connected by two flexible methylene linkers at the C3 and C3' positions of BINOL, respectively. To further illustrate the importance of the C-2 hydrogen of the imidazolium nucleus for binding guest molecules, an analogue (*R*)-2 of receptor (*R*)-1, in which the C-2 hydrogen of imidazolium is substituted by a methyl group, was synthesized for comparison. As demonstrated in Scheme 2, the syntheses of receptors (*R*)-1 and (*R*)-2 were accomplished by a straightforward process starting from (*R*)-2,2'-dimethoxy-1,1'-binaphthyl [(*R*)-6]. Formylation of (*R*)-6 in the presence of *n*BuLi and DMF afforded (*R*)-2,2'-dimethoxy-1,1'-binaphthyl-3,3'-dicarbaldehyde [(*R*)-7],¹⁷ which was subjected to reduction with NaBH₄ and then chlorination with SOCl₂.¹⁸ The resulting (*R*)-3,3'-dichloromethyl-2,2'-dimethoxy-1,1'-binaphthyl [(*R*)-9] was deprotected with BBr₃ to afford (*R*)-3,3'-dichloromethyl-1,1'-bi-2-naphthol [(*R*)-10] and coupled with imidazole to give (*R*)-3,3'-di(1*H*-imidazol-1-ylmethyl)-2,2'-dimethoxy-1,1'-binaphthyl [(*R*)-11], respectively. The desired receptors (*R*)-1 and (*R*)-2 were finally obtained by refluxing (*R*)-10 with *N*-methyl-1*H*-imidazole and 1,2-dimethyl-1*H*-imidazole in acetonitrile, respectively.

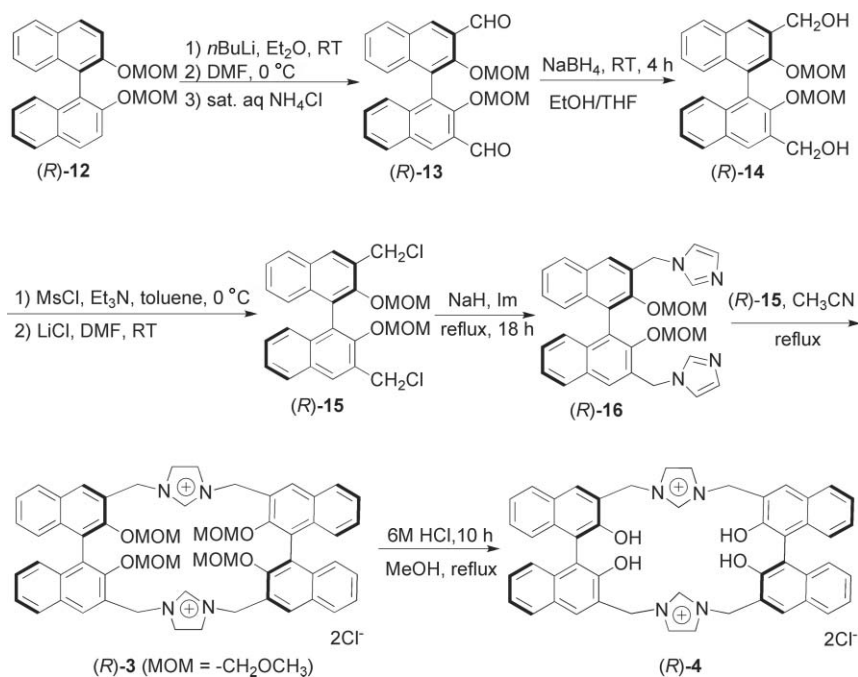
It is well known that, for enantiodiscriminating purposes, reducing the flexibility of the receptor may lead to the enhancement of chiral recognition capability. Subsequently, the macrocyclic compounds (*R*)-3, (*R*)-4 and (*R*)-5 with a defined cavity were synthesized. The binaphthyl linker closes the open structure of (*R*)-1, thus not only reducing the flexibility and enhancing the preorganization, but also furnishing enough stereomatching interaction sites between the host and guest. The cyclization was performed by coupling (*R*)-9 with (*R*)-11 to afford the macrocyclic (*R*)-5 in acetonitrile under high dilute conditions. It is noteworthy that initial attempts to synthesize the macrocyclic receptor (*R*)-4 *via* the deblocking of the methyl protecting groups of (*R*)-5 with BBr₃ were unsuccessful. As a consequence, we chose the readily available (*R*)-2,2'-dimethoxymethoxy-1,1'-binaphthyl [(*R*)-12] as a starting material to prepare this cyclic compound. As shown in Scheme 3, the synthetic method of (*R*)-3 was similar to that of (*R*)-5 by cyclizing (*R*)-3,3'-dichloromethyl-2,2'-dimethoxymethoxy-1,1'-binaphthyl [(*R*)-15]¹⁹ with (*R*)-3,3'-di(1*H*-imidazol-1-ylmethyl)-2,2'-dimethoxymethoxy-1,1'-binaphthyl [(*R*)-16]. Removal of the methoxymethyl (MOM) group from (*R*)-3 produced the expected receptor (*R*)-4 in the presence of 6 M HCl.

X-Ray structure of (*R*)-5

After numerous attempts, colorless block crystals were luckily obtained by slow diffusion of diethyl ether into a solution of (*R*)-5 in methanol for several days, and its X-ray analysis established the molecular structure of (*R*)-5.^{20,21} The structural geometry revealed that the central cavity of the macrocycle is defined by two almost parallel naphthalene rings separated by approximately 6.87 Å and the dihedral angles of the two BINOL moieties are about 76° and 74°, respectively. The C-2 hydrogen atoms of two imidazolium rings are oppositely directed towards the out-of-central cavity (Fig. 1). More importantly, the two Cl⁻ ions are positioned



Scheme 2 Synthesis of binaphthyl-based imidazolium receptors (*R*)-1, (*R*)-2 and (*R*)-5.



Scheme 3 Synthesis of binaphthyl-based imidazolium receptors (R)-3 and (R)-4.

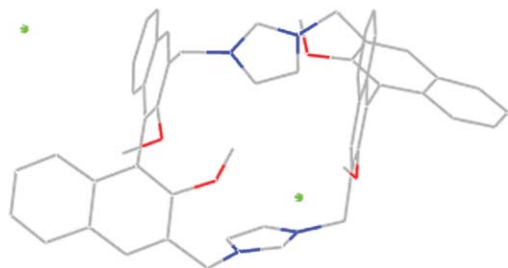


Fig. 1 X-Ray crystal structure of (R)-5. Color code: C (dark gray), N (blue), O (red), Cl (green), and H (omitted).

outside the cavity and there is no intramolecular or intermolecular $(\text{C}-\text{H})^+ \cdots \text{Cl}^-$ hydrogen bonding.

Optical spectroscopic studies of receptors (R)-1–5

The UV spectra of (R)-1, (R)-2, (R)-3, (R)-4 and (R)-5 were first investigated in HEPES buffer solutions at 1.0×10^{-5} M. As displayed in Fig. 2a, the receptors (R)-1, (R)-2, (R)-3, (R)-4 and (R)-5 gave rise to similar UV absorption bands. However, the long wavelength absorption maximum (336 nm) of the macrocyclic (R)-4 was slightly red-shifted relative to that of the open cleft (R)-1 (334 nm), implying that the macrocyclic structure of (R)-4 might restrict the rotation of the binaphthalene unit around the 1,1'-bonds and thus force them to achieve a better conjugation than the corresponding flexible acyclic compound.^{14c} In addition, the absorption maxima of the two macrocycles (R)-3 and (R)-5 were almost identical. Compared to (R)-4, the long wavelength absorption maxima of (R)-3 and (R)-5 were blue-shifted to $\lambda_{\text{max}} = 326$ nm, and at short wavelengths (220–300 nm), both (R)-3 and (R)-5 had a greatly increased intensity, which was attributed to the methoxymethyl and methyl protection of the aryl hydroxyl groups, respectively.^{14b}

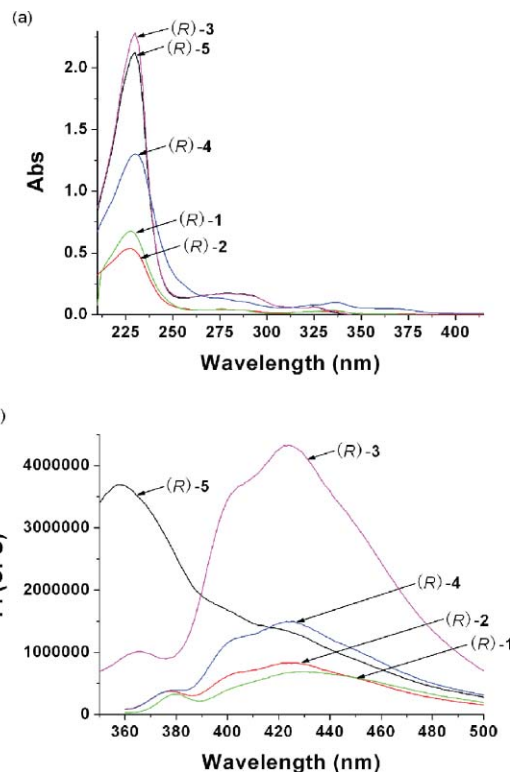


Fig. 2 (a) UV spectra of (R)-1, (R)-2, (R)-3, (R)-4 and (R)-5 in aqueous solutions (1.0×10^{-5} M). (b) Fluorescence spectra of (R)-1, (R)-2, (R)-3, (R)-4 and (R)-5 ($1 \mu\text{M}$) in aqueous solutions ($\lambda_{\text{exc}} = 336$ nm, 336 nm, 327 nm, 336 nm and 327 nm, respectively; emission slits = 5.0 nm). (R)-1: 10 mM HEPES buffer, pH 7.4; (R)-2, (R)-3, (R)-4 and (R)-5: HEPES buffered (10 mM, pH 7.4) $\text{CH}_3\text{OH}-\text{H}_2\text{O}$ (1 : 1, v/v).

Fig. 2b gave the fluorescence spectra of (R)-1, (R)-2, (R)-3, (R)-4 and (R)-5 in aqueous solutions at $1 \mu\text{M}$. The emission maximum

of (*R*)-**4** at 425 nm was similar to that of acyclic (*R*)-**1** (428 nm) with a slight blue shift. Despite similar UV spectra, (*R*)-**3** and (*R*)-**5** exhibited significant differences in emission. (*R*)-**3** displayed a fluorescence emission at 424 nm while (*R*)-**5** showed an emission peak at 358 nm. The fluorescence quantum yields of (*R*)-**3**, (*R*)-**4** and (*R*)-**5**, referenced to a quinine sulfate solution in 1 M H₂SO₄ ($\Phi_F = 0.55$),^{14c} were determined, and found to be 5.78, 1.24 and 4.81%, respectively. As the macrocyclic (*R*)-**4** had a lower quantum yield than those of (*R*)-**3** and (*R*)-**5**, we rationalized that the acidic aryl hydroxyl groups of (*R*)-**4** might diminish the fluorescence due to intra- or intermolecular hydrogen bonds and/or proton transfer at the excited states.^{14b}

Guest binding studies with L-amino acids

The binding properties of receptors (*R*)-**1**–**5** with various natural α -amino acids were investigated by UV and fluorescence titration experiments in aqueous solutions under the physiological pH value (pH 7.4). Fig. 3a shows the UV absorption changes of (*R*)-**1** upon addition of a variety of α -amino acids including L-cysteine (L-Cys), L-tryptophan (L-Trp), L-phenylalanine (L-Phe), L-tyrosine (L-Tyr), L-histidine (L-His), L-serine (L-Ser), L-proline (L-Pro), L-alanine (L-Ala), glycine (Gly), L-glutamic acid (L-Glu) and L-valine (L-Val) in a HEPES-buffered aqueous medium. The experimental results demonstrated that receptor (*R*)-**1** had more significant recognition ability towards L-Trp over the other amino acids examined.

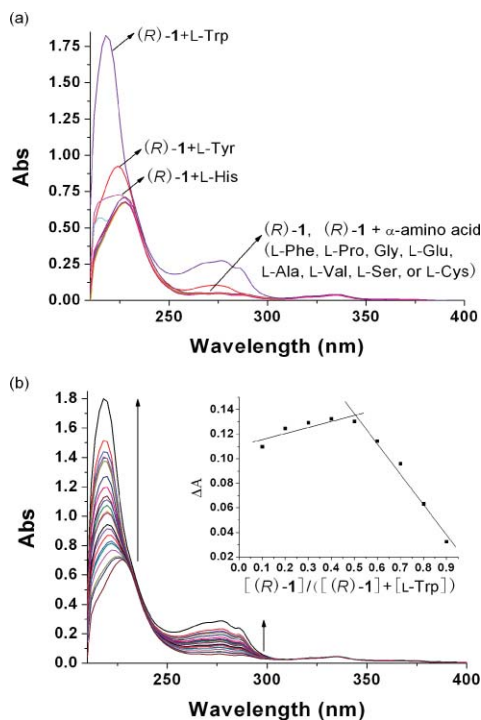


Fig. 3 (a) UV absorption changes of (*R*)-**1** (1.0×10^{-5} M) upon addition of various natural amino acids (5 equiv.) in aqueous media (10 mM HEPES buffer, pH 7.4). (b) UV titrations of (*R*)-**1** (1.0×10^{-5} M) upon addition of L-Trp in aqueous solutions (10 mM HEPES buffer, pH 7.4). Inset: the Job's plot; the total concentration of ($[(R)-1] + [L-Trp]$) was 10 μ M.

Tryptophan, an essential amino acid, plays a crucial part in biological processes such as protein biosynthesis, animal growth and

plant development.²² The recognition of tryptophan is meaningful because it serves as the precursor for serotonin, a neurotransmitter that helps the body regulate appetite, sleep patterns, and mood. It has also been implicated as a possible cause of schizophrenia due to its improper metabolism under *in vivo* conditions,²³ and lack of it also be the cause of pellagra. Although considerable endeavors have been devoted to deal with the detection of tryptophan, studies on the use of the UV and fluorometric assays for this purpose still remain sparse.^{24,25} To further explore the ability of (*R*)-**1** as a potential probe, UV titrations of (*R*)-**1** with an increase in addition of L-Trp were first performed in a HEPES buffer solution at pH 7.4. As shown in Fig. 3b, free (*R*)-**1** gave an absorption maximum at 228 nm. Upon addition of L-Trp from 0–5 equiv., the λ_{max} underwent a blue shift to 218 nm along with a dramatic increase in absorbance, and a concomitant regular increase in absorbance at 276 nm was also observed, which indicated the formation of a complex between L-Trp and a receptor in the ground state. Job analysis for the complexation of (*R*)-**1** and L-Trp at 228 nm shown in the inset of Fig. 3b corroborated the 1 : 1 binding stoichiometry.

Next, the selective and sensitive sense of (*R*)-**1** towards the eleven L-amino acids was studied using fluorescence changes in an aqueous solution of physiological pH (7.4) when excited at 369 nm.²⁶ The detailed variations in fluorescence intensity in the presence of different amino acids are explained in Fig. 4a. A distinct fluorescence enhancement upon addition of L-Trp was detected, while the other amino acids induced much smaller or negligible changes, which was in good agreement with the results from the UV spectra. Subsequently, fluorescence titration

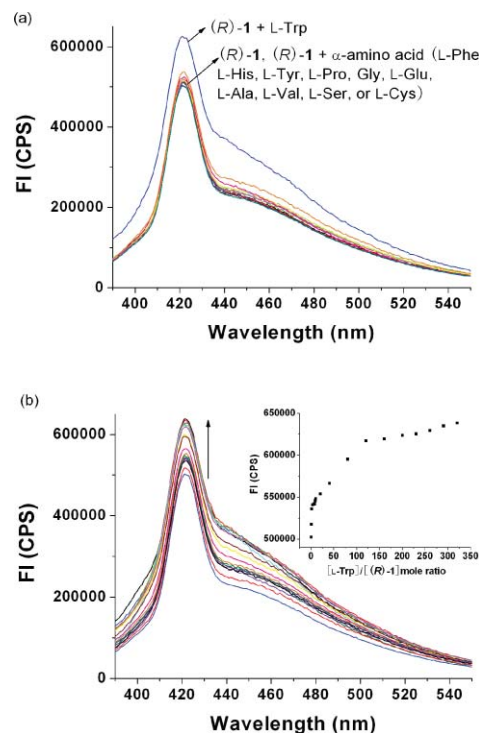


Fig. 4 (a) Changes in fluorescence intensity of (*R*)-**1** (1μ M) upon addition of 200 equiv. of various natural amino acids in H₂O (10 mM HEPES buffer, pH 7.4) ($\lambda_{exc} = 369$ nm, slits = 5.0 nm). (b) Fluorescence spectra changes of (*R*)-**1** (1μ M) with L-Trp (0–320 μ M) in H₂O (10 mM HEPES buffer, pH 7.4). Inset: fluorescence intensity at 422 nm versus equivalents of L-Trp.

Table 1 Association constants (M^{-1}) for the complexes of (*R*)-**1** with different nature amino acids in aqueous solutions (10 mM HEPES buffer, pH = 7.4) at 25 °C

Amino acid	K/M^{-1} ^a	Amino acid	K/M^{-1} ^a
L-Trp	$(1.73 \pm 0.01) \times 10^4$	L-Pro	nd ^b
L-Phe	$(7.28 \pm 0.90) \times 10^3$	Gly	$(2.17 \pm 0.83) \times 10^3$
L-Tyr	$(2.96 \pm 0.27) \times 10^3$	L-Glu	nd ^b
L-His	$(3.79 \pm 0.91) \times 10^3$	L-Ala	nd ^b
L-Val	$(6.06 \pm 0.51) \times 10^2$	L-Ser	nd ^b
L-Cys	$(1.45 \pm 0.45) \times 10^3$		

^a All error values were obtained by the results of Benesi–Hildebrand plots, and the correlation coefficient (*R*) of linear fitting is over 0.99. ^b Not determined because of negligible changes in the fluorescence spectra.

experiments of (*R*)-**1** towards these amino acids were carried out. As illustrated in Fig. 4b, taking L-Trp as a representative example, the fluorescence emission intensity of a 1 μ M solution of (*R*)-**1** at 422 nm gradually enhanced with an increase in the concentration of L-Trp, which followed the linear Benesi–Hildebrand expression (Fig. S4b, ESI[†]):²⁷

$$\frac{I_0}{I - I_0} = \frac{b}{a - b} \left\{ \frac{1}{K[M]} + 1 \right\}$$

where I_0 is the fluorescence intensity of the receptor in the absence of guest; I is the fluorescence intensity in the presence of guest; $[M]$ is the concentration of guest; K is the association constant between receptor and guest. In the equation, both a and b are constants. The association constant K values of (*R*)-**1** with the eleven amino acids are listed in Table 1, and they obviously display a better selectivity towards L-Trp than the others.

To shed light on the possible origin of the significant performance of (*R*)-**1**, (*R*)-**2** lacking the C-2 hydrogen of the imidazolium nucleus was next chosen for comparison. It was found that addition of various amino acids to (*R*)-**2** showed smaller or negligible changes in the fluorescence spectra (Fig. 5). These results clearly indicated the key role of the C-2 hydrogen atom of the imidazolium ring, which was further supported by the following modeling studies.

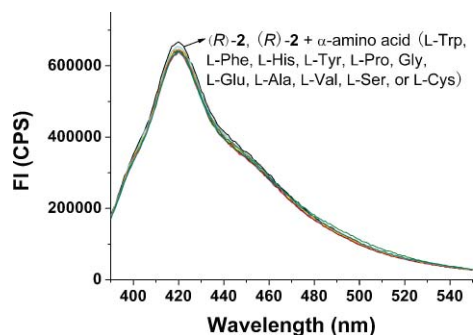


Fig. 5 Changes in fluorescence intensity of (*R*)-**2** (1 μ M) upon addition of 200 equiv. of various natural amino acids ($\lambda_{exc} = 369$ nm, slits = 5.0 nm) in HEPES buffered (10 mM, pH 7.4) CH_3OH-H_2O (1 : 1, v/v).

To investigate the binding properties of (*R*)-**4** towards α -amino acids, the CH_3OH-H_2O system (1 : 1, 10 mM HEPES buffer, pH 7.4) was employed to ensure that the receptor was completely

dissolved in an aqueous medium in the titration experiments. The emission properties of (*R*)-**4** showed interesting changes with a variety of α -amino acids (Fig. S1, ESI[†]). A remarkable fluorescence enhancement was observed upon addition of L-Trp, whereas L-Tyr displayed a fluorescent quenching effect. The result clearly demonstrated a unique binding ability of the macrocyclic (*R*)-**4** towards L-Trp. In contrast, the receptor (*R*)-**3**, in which the four aryl hydroxyl groups are protected by the MOM groups, distinctly showed an inferior selectivity towards amino acids, as it was notably in response to several aromatic amino acids (*i.e.*, L-Tyr, L-Phe, L-His, and L-Trp) (for fluorescent spectra, see Fig. S2, ESI[†]). Interestingly, (*R*)-**3** exhibited enhanced fluorescent properties towards L-Tyr, implying that the fluorescent quenching effect of L-Tyr toward (*R*)-**4** might arise from the intermolecular hydrogen bonds between the aryl hydroxyl groups of host and guest at the excited states.^{14b} Similar experiments employing the Me-protected macrocyclic (*R*)-**5** were also conducted when excited at 292 nm. Thus, the receptor (*R*)-**5** also showed selective recognition ability toward L-Trp (Fig. S3, ESI[†]).

The fluorescence ratios $(I - I_0)/I_0$ of (*R*)-**1**, (*R*)-**2**, (*R*)-**3**, (*R*)-**4** and (*R*)-**5** were displayed in the presence of 200 equiv. of various amino acids. As shown in Fig. 6, except for (*R*)-**2**, the other four receptors exhibited significant enhancement of the fluorescence intensity towards L-Trp. However, (*R*)-**3**, (*R*)-**4** and (*R*)-**5** could also exhibit small spectral changes with some aromatic amino acids such as L-Tyr, L-Phe and L-His, which might interfere in the specific recognition of L-Trp. In contrast, the cleft-like receptor (*R*)-**1** with high flexibility could adopt a predominant configuration to bind the unique guest molecule, and thus was indicative of a better selectivity for L-Trp among various amino acids. This implied that the preorganization of the receptive sites of the host sufficiently utilized the multiple hydrogen-bonding interactions only with structurally complementary guest molecules (*i.e.*, (*R*)-**1** and L-Trp). In addition to the electrostatic interactions between the carboxyl group of L-Trp and the imidazolium moiety, these subtle interactions led to the formation of a stable complex between (*R*)-**1** and L-Trp.

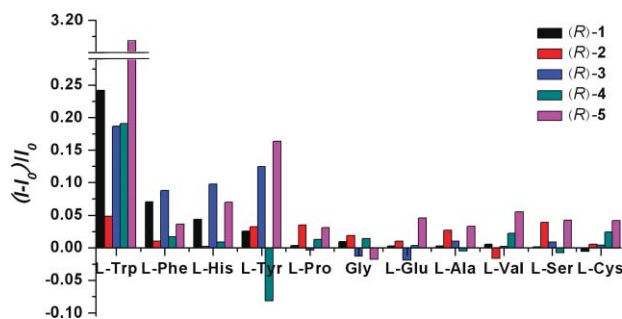


Fig. 6 Fluorescence ratios $(I - I_0)/I_0$ of receptors (*R*)-**1**, (*R*)-**2**, (*R*)-**3**, (*R*)-**4** and (*R*)-**5** (1 μ M) upon addition of 200 equiv. of L-amino acids in aqueous solutions.

Based on the Benesi–Hildebrand-type analysis,²⁷ the measured emission $[I_0/(I - I_0)]$ varied as a function of $1/[L-Trp]$ in a linear relationship, indicating the 1 : 1 stoichiometry between L-Trp and the receptor (*R*)-**1**, (*R*)-**2**, (*R*)-**3**, (*R*)-**4** or (*R*)-**5** (Fig. S4, S5, S6, S7 and S8, ESI[†]). From these plots, the association constant K values of (*R*)-**1**, (*R*)-**2**, (*R*)-**3**, (*R*)-**4** and (*R*)-**5** for L-Trp were

Table 2 Association constants (M^{-1}) for the complexes of tryptophan (Trp) with receptors in aqueous solutions (10 mM HEPES buffer, pH = 7.4) at 25 °C

Receptor	K_{L-Trp}/M^{-1}^a	K_{D-Trp}/M^{-1}^a	K_{D-Trp}/K_{L-Trp}
(<i>R</i>)-1	$(1.73 \pm 0.01) \times 10^4$	$(1.09 \pm 0.03) \times 10^4$	0.6
(<i>R</i>)-2	$(8.04 \pm 1.62) \times 10$	$(8.34 \pm 2.20) \times 10$	1.0
(<i>R</i>)-3	$(2.89 \pm 0.12) \times 10^3$	$(1.79 \pm 0.03) \times 10^4$	6.2
(<i>R</i>)-4	$(4.78 \pm 0.07) \times 10^3$	$(3.38 \pm 0.13) \times 10^3$	0.7
(<i>R</i>)-5	$(2.59 \pm 0.12) \times 10^3$	$(5.42 \pm 0.02) \times 10^3$	2.1

^a All error values were obtained by the results of Benesi–Hildebrand plots, and the correlation coefficient (*R*) of linear fitting is over 0.99.

determined to be 1.73×10^4 , 8.04×10 , 2.89×10^3 , 4.78×10^3 and $2.59 \times 10^3 M^{-1}$, respectively (Table 2). Clearly, these results explain that (*R*)-1 bound L-Trp with approximately 215, 6, 4 and 7-fold stronger association constants than (*R*)-2, (*R*)-3, (*R*)-4 and (*R*)-5, respectively.

The 1:1 coordination mode was further confirmed by the electrospray ionization (ESI) mass spectra. Five complexes of L-Trp with (*R*)-1, (*R*)-2, (*R*)-3, (*R*)-4 and (*R*)-5 in a 1:1 ratio showed the peaks at *m/z* 716.8, 744.5, 1232.2, 996.4 and 1089.3, which could be assigned to the species [(*R*)-1 – Cl[−] + L-Trp + H]⁺, [(*R*)-2 – Cl[−] + L-Trp + H]⁺, [(*R*)-3 + L-Trp + Na]⁺, [(*R*)-4 – Cl[−] + L-Trp – H]⁺ and [(*R*)-5 + L-Trp + H]⁺, respectively (see Fig. S15, S16, S17, S18, and S19, ESI[†]).

Molecular modeling structures

Theoretical calculations were performed to better understand the mechanism of interaction between (*R*)-1 and Trp. The molecular modeling structures were fully-optimized at the HF/STO-3G* level using the Gaussian 03 program. As depicted in Fig. 7a, these calculations revealed a 1:1 stoichiometry for the multiple hydrogen-bonded complex between (*R*)-1 and L-Trp, in which the strong interactions between the carboxyl group of L-Trp and the chiral ligand, including two C2-hydrogen atoms of two imidazolium rings and one aryl hydroxyl group, were observed with three hydrogen bond distances ranging from 1.589–1.670 Å. The dihedral angle of the BINOL moiety was significantly distorted from its normal angle due to such strong interactions. In addition to these interactions, the additional hydrogen-bonds formed between the indole unit (NH) of L-Trp and the other hydroxyl group of the host *via* a water molecule, further stabilizing the L-Trp-ligand complex. In the sense of computational chemistry, the additional hydrogen bonds would favor the coordination of L-Trp with the receptor (*R*)-1 as compared to other amino acids investigated. The calculations also showed that the D-configuration complex is close to its L-analogue in relative energy. Thus, the receptor (*R*)-1 would result in a poor enantioselectivity for the recognition of the enantiomers of Trp, which was in agreement with the experimental results.

Chiral recognition of tryptophan

Subsequently, all of five binaphthyl-based imidazolium receptors (*R*)-1–5 were investigated as fluorescent chemosensors for chiral recognition of the two enantiomers of tryptophan (Trp) (Fig. S14, ESI[†]). The acyclic (*R*)-1 displayed a small K_D/K_L value for Trp while the acyclic (*R*)-2 lacking the C-2 hydrogen of the imidazolium

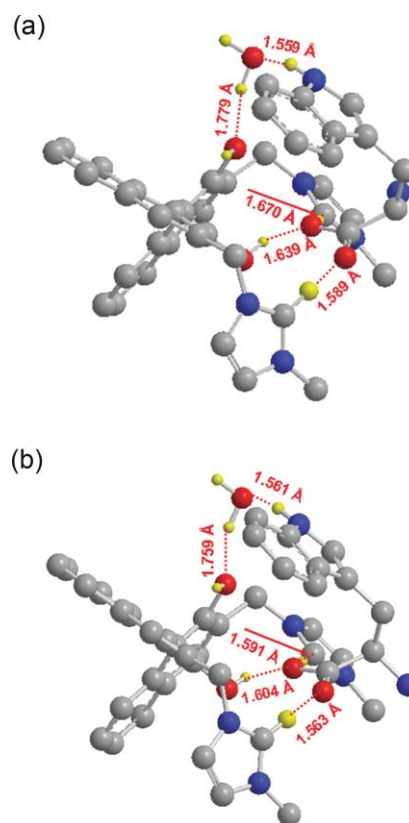


Fig. 7 Optimized geometries of (a) (*R*)-1-L-Trp complex and (b) (*R*)-1-D-Trp complex at the HF/STO-3G* level. Color code: C (dark gray), N (blue), H (yellow), and O (red). The hydrogen bond interactions (Å) are shown as red dashed lines. Part of hydrogen atoms are omitted for clarity.

ring almost did not give enantioselectivity (Table 2). Clearly, these acyclic receptors are more flexible to lead to the lack of the degree of preorganization. This loss makes the association process less favorable in the enantiodiscrimination. In contrast, the Me-protected macrocycle (*R*)-5 gave a moderate enantioselective recognition for the two enantiomers of Trp ($K_D/K_L = 2.1$), and the MOM protecting macrocyclic receptor (*R*)-3 showed an enhanced enantioselectivity with a K_D/K_L value as high as 6.2. We rationalized that the increase is likely ascribed to a reduced cavity size to lead to a better fit, thus making the enantiodiscriminating complement of interactions more effective. Interestingly, the D/L selectivities of (*R*)-3 and (*R*)-5 towards Trp are opposite to those of (*R*)-1 and (*R*)-4, even though all receptors bear similar binding units. We speculated that (*R*)-3 presumably adopts the geometry of “pocket” formed by the four MOM groups to bind Trp in the recognition process. In this pocket, all the MOM groups take the same orientation out of the macrocycle.

To further explain the formation of complexes and the main binding interactions, the ¹H NMR titration experiments were first undertaken using the macrocyclic (*R*)-3 in CD₃OD–D₂O (1:1, v/v). Unfortunately, the proton resonances of (*R*)-3 appeared to lose resolution due to the undesirable solubility. This situation deteriorated through addition of tryptophan, and no signal could then be successfully used to track the changes that were occurring upon binding. Thus, we chose the water-soluble acyclic (*R*)-1. In Fig. 8, upon addition of an equimolar amount of L- or

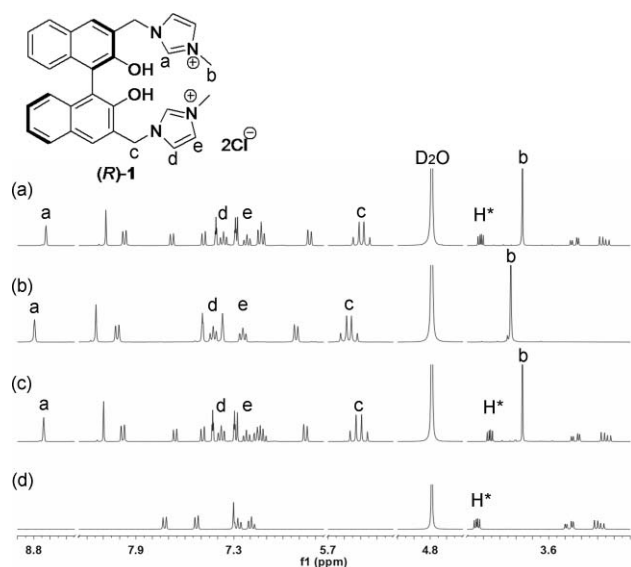


Fig. 8 Partial ^1H NMR spectra of (*R*)-**1** and its complex at 25 °C in D_2O : (a) (*R*)-**1** + 1.0 equiv of D-Trp; (b) (*R*)-**1**; (c) (*R*)-**1** + 1.0 equiv of L-Trp; (d) racemic tryptophan.

D-Trp into the D_2O solution of (*R*)-**1**, significant ^1H NMR spectral changes were observed. For example, the imidazolium C2–H peaks underwent upfield shifts by 0.06 ppm to 8.74 and 0.07 ppm to 8.73 for L- and D-Trp, respectively, indicating that one of the interactions between the host and guest happened through the hydrogen bonds between the C₂–H of the imidazolium rings and the carboxylate. The H₄ and H₅ protons of the imidazolium rings, as well as the benzyl and methyl protons, also gave rise to obvious upfield shifts. Furthermore, the peak for the methenyl proton (H*) of free tryptophan that appeared at 4.02 ppm moved to 3.95 ppm and 4.00 ppm, while 1 equiv. of L-Trp and D-Trp were respectively added to (*R*)-**1**, which afforded a clue for the enantioselective recognition toward the enantiomers of Trp.

Conclusions

In summary, we have synthesized a type of 1,1'-binaphthyl-based imidazolium chemosensor for the highly selective recognition of tryptophan (Trp) among the eleven α -amino acids in aqueous solutions *via* synergistic effects of multiple hydrogen bonding and electrostatic interactions. The structurally open receptor (*R*)-**1** exhibits the more significant selectivity and affinity towards L-Trp than the other receptors (*R*)-**2**–**5**. The macrocyclic (*R*)-**3** exhibits a remarkable chiral recognition capability for the two enantiomers of tryptophan with a K_D/K_L of 6.2 despite an inferior selectivity towards a variety of aromatic amino acids. Through the methylation of the C-2 hydrogen of the imidazolium nucleus of (*R*)-**1**, the role of the imidazolium ring was identified as a strong hydrogen-bond donor in the selective recognition process. These results highlight that the structural complementation between host and guest, the relative flexibility and the good preorganization property of the host are responsible for the good selective recognition. We believe that the design strategy is helpful for the development of various sensors and would be potentially useful for detecting the enantiomers of Trp in biomedical applications.

Experimental section

General remarks

^1H NMR spectra were obtained with a Bruker AV-300 (300 MHz), a Bruker AV-400 (400 MHz), a Varian Inova-400 (400 MHz) or a Varian Inova-600 (600 MHz) spectrometer, while ^{13}C NMR spectra were also recorded with a Bruker AV-300 (75 MHz), a Bruker AV-400 (100 MHz), a Varian Inova-400 (100 MHz) or a Varian Inova-600 (150 MHz) spectrometer. The ^1H NMR chemical shifts were measured relative to tetramethylsilane, CDCl_3 or $\text{DMSO}-d_6$ as the internal reference, while the ^{13}C NMR chemical shifts were recorded with CDCl_3 , $\text{DMSO}-d_6$ or CD_3OD as the internal standard. Mass spectra were obtained on a BioTOF Q or a Finnigan-LCQ^{DECA} instrument. The ESI-TOF mass spectra were recorded with a Waters Q-ToF premier instrument, and the optical rotations were determined with a AUTOPOL V polarimeter. Elemental analyses were performed with a CARLO ERBA1106 instrument. Melting points were determined with XRC-1 and are uncorrected.

X-Ray crystallography

X-Ray single-crystal diffraction data for (*R*)-**5** was collected on a Bruker SMART 1000 CCD areadetector diffractometer at 100 K with graphite monochromated Mo-K α radiation ($\lambda = 0.71073 \text{ \AA}$) with ω scan mode. The structure was solved by direct methods using the SHELXS program and refined by full-matrix least-squares methods with SHELXL.²⁸ All non-hydrogen atoms were located in successive difference Fourier syntheses and refined with anisotropic thermal parameters on F². Hydrogen atoms were included in calculated positions and refined with constrained thermal parameters riding on their parent atoms.

Materials

(*R*)-1,1'-Bi-2-naphthol [(*R*)-BINOL] (>99% ee) was purchased from Lian YunGang Chiral Chemicals (China) Co., Ltd. All liquid reagents were distilled before use, while the others were used without further purification. Solvents were dried by heating at reflux for at least 24 h over CaH_2 (dichloromethane and DMF) or sodium/benzophenone (tetrahydrofuran, toluene and diethyl ether) and were freshly distilled prior to use. Except where noted, commercial reagents were used as received without further purification. Unless otherwise indicated, all syntheses and manipulations were carried out under a dry nitrogen atmosphere. *n*BuLi in Et_2O was prepared according to the literature.²⁹ Compounds (*R*)-**6**, (*R*)-**7** and (*R*)-**8** were synthesized according to the procedure reported by Stock and Kellogg.¹⁷ Compounds (*R*)-**12**, (*R*)-**13**, (*R*)-**14** and (*R*)-**15** were prepared according to literature methods.¹⁹

Procedures for the preparation of receptors (*R*)-**1**–**5**

(*R*)-3,3'-Dichloromethyl-2,2'-dimethoxy-1,1'-binaphthyl [(*R*)-9**].** To a cooled (0 °C) solution of (*R*)-**8** (5.99 g, 16 mmol) in anhydrous CH_2Cl_2 (80 mL) was added dropwise SOCl_2 (23.2 mL, 320 mmol). The reaction mixture was then allowed to warm to room temperature and stirring was continued for 12 h. Volatiles were removed under reduced pressure to afford the crude product. (*R*)-**9** was obtained in 95% yield (6.25 g) as a white solid after

purification by column chromatography on silica gel eluting with petroleum ether–CH₂Cl₂ (1 : 1). M.p. 92–95 °C; ¹H NMR (300 MHz, CDCl₃): δ 3.33 (s, 6 H), 4.81 (dd, *J* = 11.5 Hz, 11.4 Hz, 4 H), 7.18 (d, *J* = 8.4 Hz, 2 H), 7.25–7.31 (m, 2 H), 7.39–7.45 (m, 2 H), 7.89 (d, *J* = 8.1 Hz, 2 H), 8.09 (s, 2 H) ppm; ¹³C NMR (75 MHz, CDCl₃): δ 42.2, 61.4, 124.5, 125.3, 125.7, 127.1, 128.2, 130.4, 131.0, 131.1, 134.4, 154.7 ppm; MS (ESI⁺) *m/z*: 411 [M]⁺.

(*R*)-3,3'-Dichloromethyl-1,1'-bi-2-naphthol [(*R*)-10]. Compound (*R*)-**9** (1.23 g, 3 mmol) was placed in a 100 mL flame-dried Schlenk flask, and anhydrous CH₂Cl₂ (75 mL) was then added under nitrogen. To a cooled (0 °C) solution, BBr₃ (1.0 M in CH₂Cl₂, 8 mL, 8 mmol) was added over a period of 30 min. After the mixture was warmed to room temperature and stirred for 12 h, a saturated NaHCO₃ solution (15 mL) was carefully added at 0 °C to quench the reaction. The neutralized mixture was poured into water (100 mL) and was extracted with CH₂Cl₂ (3 × 50 mL). The combined organic layers were dried over Na₂SO₄, and concentrated *in vacuo*. Finally, the resulting residue was recrystallized in petroleum ether–acetone (5 : 1) to give (*R*)-**10** as pale white needle-like crystals (0.87 g, 86%). M.p. 205–207 °C; [α]_D²⁰ = +106.8 (*c* = 0.25, CH₃OH); ¹H NMR (400 MHz, CDCl₃): δ 4.78 (dd, *J* = 10.0 Hz, 10.4 Hz, 4 H), 5.34 (s, 2H), 7.08 (d, *J* = 8.4 Hz, 2 H), 7.30 (t, *J* = 7.2 Hz, 2 H), 7.38 (t, *J* = 8.0 Hz, 2 H), 7.88 (d, *J* = 8.0 Hz, 2 H), 8.08 (s, 2 H) ppm; ¹³C NMR (100 MHz, CDCl₃): δ 28.8, 111.4, 124.1, 124.7, 126.6, 128.2, 128.6, 129.2, 132.3, 133.4, 150.8 ppm; HRMS (ESI-TOF) *m/z*: calcd for [M–2Cl–H]⁺: 311.1072; found: 311.1062.

Preparation of receptor (*R*)-1. To a solution of (*R*)-**10** (767 mg, 2 mmol) in 10 mL of acetonitrile, *N*-methyl-1*H*-imidazole (0.5 mL, 6 mmol) in acetonitrile (10 mL) was added dropwise. The mixture was heated under reflux for 36 h. After cooling to room temperature, the solvent was concentrated *in vacuo*. The compound was purified by column chromatography on silica gel, eluting with CH₂Cl₂–CH₃OH (gradient 10 : 1 to 3 : 1) to CH₃OH, to afford (*R*)-**1** as a pale yellow solid (495 mg, 45%). M.p. 185–187 °C; [α]_D²⁰ = +45.6 (*c* = 0.25, CH₃OH); ¹H NMR (400 MHz, DMSO-*d*₆): δ 3.83 (s, 6H), 5.53 (dd, *J* = 14.4 Hz, 14.4 Hz, 4H), 6.81 (d, *J* = 8.4 Hz, 2H), 7.22 (t, *J* = 7.2 Hz, 2H), 7.31 (t, *J* = 8.0 Hz, 2H), 7.70 (s, 2H), 7.76 (s, 2H), 7.91 (d, *J* = 8.0 Hz, 2H), 8.07 (s, 2H), 9.10 (s, 2H) ppm; ¹³C NMR (100 MHz, DMSO-*d*₆): δ 36.3, 49.6, 115.0, 123.2, 123.9, 124.0, 124.2, 124.5, 127.5, 128.6, 128.8, 131.6, 134.9, 137.2, 152.5 ppm; MS (ESI) *m/z*: 475 [M–2Cl–H]²⁺; Anal. Calcd for C₃₀H₃₄Cl₂N₄O₂: C, 65.10; H, 6.19; N, 10.12. Found: C, 64.84; H, 6.30; N, 9.94.

Preparation of receptor (*R*)-2. To a solution of (*R*)-**10** (383 mg, 1 mmol) in 5 mL of acetonitrile, 1,2-dimethyl-1*H*-imidazole (288 mg, 3 mmol) in acetonitrile (5 mL) was added dropwise. The mixture was heated under reflux for 36 h. After cooling to room temperature, the solvent was concentrated *in vacuo*. The compound was purified by column chromatography on silica gel, eluting with CH₂Cl₂–CH₃OH (gradient 10 : 1 to 3 : 1) to CH₃OH, to give (*R*)-**2** as a pale yellow solid (242 mg, 42%). M.p. 214–216 °C; [α]_D²⁰ = +24.8 (*c* = 0.25, CH₃OH); ¹H NMR (400 MHz, DMSO-*d*₆): δ 2.69 (s, 6H), 3.83 (s, 6H), 5.54 (s, 4H), 6.82 (d, *J* = 8.4 Hz, 2H), 7.22 (t, *J* = 8.4 Hz, 2H), 7.31 (t, *J* = 8.0 Hz, 2H), 7.65 (d, *J* = 2.0 Hz, 2H), 7.70 (d, *J* = 2.0 Hz, 2H), 7.86 (s, 2H), 7.90 (d, *J* = 8.0 Hz, 2H), 8.91 (s, 2H) ppm; ¹³C NMR (100 MHz,

DMSO-*d*₆): δ 10.1, 35.4, 48.3, 114.6, 121.9, 122.8, 123.8, 124.3, 127.3, 128.6, 128.7, 130.2, 134.6, 145.2, 152.3 ppm; MS (ESI) *m/z*: 592 [M+NH₄]⁺; Anal. Calcd for C₃₂H₃₈Cl₂N₄O₂: C, 66.09; H, 6.59; N, 9.63. Found: C, 65.82; H, 6.45; N, 9.49.

(*R*)-3,3'-Di(1*H*-imidazol-1-ylmethyl)-2,2'-dimethoxy-1,1'-binaphthyl [(*R*)-11]. A flame-dried three-necked flask was charged with imidazole (1.85 g, 27 mmol) and NaH (60% in mineral oil, 2.23 g, 54 mmol) under nitrogen, and then dry THF (50 mL) was added at 0 °C. After the mixture was stirred for 3 h at room temperature, a solution of (*R*)-**9** (3.73 g, 9.1 mmol) in 50 mL of THF was then added dropwise under reflux, and the resulting mixture was stirred at the same temperature for 18 h. Thereafter, water (40 mL) was slowly added at 0 °C, and the mixture was stirred for 20 min and then concentrated under reduced pressure. Dichloromethane (80 mL) was added to the residue and the biphasic mixture was stirred until the solid was dissolved. The organic layer was separated, and the aqueous layer was extracted with CH₂Cl₂ (2 × 40 mL). The combined organic layers were washed with brine (40 mL), dried over Na₂SO₄ and concentrated *in vacuo*. The crude product was purified by silica gel flash column chromatography eluting with CH₂Cl₂–CH₃OH (20 : 1) to give (*R*)-**11** as white powder (3.72 g, 87%). M.p. 75–77 °C; [α]_D¹⁹ = –50 (*c* = 0.25, CH₃OH); ¹H NMR (600 MHz, CDCl₃): δ 3.03 (s, 6H), 5.33 (dd, *J* = 15.0 Hz, 15.6 Hz, 4 H), 7.05 (s, 2H), 7.13 (s, 2H), 7.15 (d, *J* = 8.4 Hz, 2H), 7.27–7.30 (m, 2H), 7.41–7.44 (m, 2H), 7.63 (s, 2H), 7.67 (s, 2H), 7.83 (d, *J* = 7.8 Hz, 2H) ppm; ¹³C NMR (150 MHz, CDCl₃): δ 47.0, 60.6, 119.5, 124.0, 125.5, 127.2, 128.1, 129.1, 129.6, 129.8, 130.2, 134.1, 137.7, 154.2 ppm; MS (ESI) *m/z*: 475 [M+H]⁺.

(*R*)-3,3'-Di(1*H*-imidazol-1-ylmethyl)-2,2'-dimethoxymethoxy-1,1'-binaphthyl [(*R*)-16]. To a flame-dried three-necked round-bottomed flask charged with imidazole (1.24 g, 18.2 mmol) and NaH (in 60% oil dispersion, 1.50 g, 36.3 mmol) was added dry THF (50 mL) with stirring at 0 °C under nitrogen. The resulting reaction mixture became a white suspension after being stirring for 3 h at room temperature. A solution of (*R*)-**15** (2.85 g, 6.1 mmol) in 50 mL of THF was then added dropwise under reflux, and the resulting mixture was stirred at the same temperature for 18 h. Thereafter, water (50 mL) was slowly added at 0 °C, and the mixture was stirred for 20 min and then concentrated under reduced pressure. Dichloromethane (80 mL) was added to the residue and the biphasic mixture was stirred until the solid was dissolved. The organic layer was separated, and the aqueous layer was extracted with CH₂Cl₂ (2 × 40 mL). The combined organic layers were washed with brine (40 mL), dried over Na₂SO₄, and concentrated *in vacuo*. The crude product was purified by silica gel flash column chromatography eluting with CH₂Cl₂–CH₃OH (25 : 1) to give (*R*)-**16** as pale yellow powder (2.65 g, 82%). M.p. 143–145 °C; [α]_D²⁰ = –90.4 (*c* = 0.25, CH₃OH); ¹H NMR (300 MHz, CDCl₃): δ 3.10 (s, 6H), 4.36 (dd, *J* = 5.9 Hz, 6.0 Hz, 4 H), 5.41 (dd, *J* = 16.0 Hz, 16.0 Hz, 4 H), 7.10–7.18 (m, 6H), 7.26–7.32 (m, 2H), 7.40–7.45 (m, 2H), 7.50 (s, 2H), 7.71 (s, 2H), 7.79 (d, *J* = 8.1 Hz, 2H) ppm; ¹³C NMR (75 MHz, CDCl₃): δ 46.9, 57.1, 99.6, 119.6, 125.0, 125.7, 125.8, 127.3, 128.2, 128.5, 129.8, 130.7, 133.8, 137.8, 152.1 ppm; MS (ESI) *m/z*: 557 [M+Na]⁺; Anal. Calcd for C₃₂H₃₀N₄O₄: C, 71.88; H, 5.66; N, 10.48. Found: C, 71.91; H, 5.63; N, 10.09.

Preparation of receptor (R)-3. (R)-15 (0.89 g, 1.9 mmol) in acetonitrile (100 mL) and (R)-16 (1.01 g, 1.9 mmol) in acetonitrile (100 mL) were added dropwise to a flame-dried three-necked flask charged with 50 mL of acetonitrile with a reflux condenser at the same time during a period of 10 h. The mixture was heated under reflux for 60 h. After the resulting mixture was cooled to room temperature, the solvent was evaporated under reduced pressure. The crude compound was purified by column chromatography on silica gel, eluting with CH₂Cl₂–CH₃OH (gradient 10 : 1 to 4 : 1) to CH₃OH, to give (R)-3 as a pale white yellow solid (1.01 g, 52.9%). M.p. 188–191 °C; $[\alpha]_{\text{D}}^{20} = -156$ ($c = 0.25$, CH₃OH); ¹H NMR (400 MHz, DMSO-*d*₆): δ 3.35 (s, 12H), 4.22 (s, 8H), 5.51 (dd, $J = 14.0$ Hz, 14.0 Hz, 8H), 6.93 (d, $J = 8.4$ Hz, 4H), 7.34 (t, $J = 6.8$ Hz, 4H), 7.50 (t, $J = 8.0$ Hz, 4H), 7.78 (s, 4H), 8.06 (d, $J = 8.0$ Hz, 4H), 8.48 (s, 4H), 9.09 (s, 2H) ppm; ¹³C NMR (100 MHz, DMSO-*d*₆): δ 49.7, 56.3, 98.4, 122.7, 124.5, 125.6, 125.9, 126.7, 127.9, 128.7, 130.1, 133.8, 134.3, 135.8, 152.4 ppm; MS (ESI) m/z : 935 [M–2Cl[–]+H]²⁺; Anal. Calcd for C₅₈H₅₄N₄O₈Cl₂: C 69.25, H 5.41, N 5.57; found: C 68.88, H 5.21, N 5.43.

Preparation of receptor (R)-4. Compound (R)-3 (560 mg, 0.56 mmol) in 35 mL of methanol was stirred at reflux in the presence of 6 M HCl (10 mL) for 10 h. Most of the solvent was removed under reduced pressure and the residue was purified by column chromatography on silica gel, eluting with CH₂Cl₂–CH₃OH (gradient 10 : 1 to 4 : 1) to MeOH, to yield (R)-4 as a pale white yellow solid (161 mg, 35%). M.p. >300 °C; $[\alpha]_{\text{D}}^{20} = +40$ ($c = 0.25$, CH₃OH); ¹H NMR (400 MHz, DMSO-*d*₆): δ 5.33 (d, $J = 13.6$ Hz, 4H), 5.61 (d, $J = 14.0$ Hz, 4H), 6.76 (d, $J = 8.8$ Hz, 4H), 7.13–7.15 (m, 4H), 7.21–7.25 (m, 4H), 7.77 (s, 4H), 7.86 (d, $J = 7.6$ Hz, 4H), 8.20 (s, 4H), 9.08 (s, 2H) ppm; ¹³C NMR (100 MHz, CD₃OD): δ 50.2, 115.4, 121.8, 123.2, 123.9, 124.6, 126.7, 128.2, 128.3, 131.8, 134.9, 153.0 ppm; MS (ESI) m/z : 758 [M–2Cl[–]]²⁺; Anal. Calcd for C₅₀H₃₈N₄O₄Cl₂: C 72.37, H 4.62, N 6.75; found: C 72.01, H 4.48, N 6.56.

Preparation of receptor (R)-5. (R)-9 (1.03 g, 2.5 mmol) in acetonitrile (100 mL) and (R)-11 (1.19 g, 2.5 mmol) in acetonitrile (100 mL) were added dropwise to a flame-dried three-necked flask charged with 50 mL of acetonitrile with a reflux condenser at the same time during a period of 10 h. The mixture was heated under reflux for 60 h. After the resulting mixture was cooled to room temperature, the solvent was evaporated under reduced pressure. The crude compound was purified by column chromatography on silica gel, eluting with CH₂Cl₂–CH₃OH (gradient 10 : 1 to 4 : 1) to CH₃OH, to give (R)-5 as a pale white yellow solid (1.59 g, 71.4%). M.p. 155–160 °C; $[\alpha]_{\text{D}}^{20} = -36.4$ ($c = 0.25$, CH₃OH); ¹H NMR (400 MHz, DMSO-*d*₆): δ 2.83 (s, 12H), 5.52–5.73 (m, 8H), 6.83 (d, $J = 8.8$ Hz, 4H), 7.29 (t, $J = 7.2$ Hz, 4H), 7.45 (t, $J = 6.8$ Hz, 4H), 7.75–7.76 (m, 4H), 8.01 (d, $J = 8.0$ Hz, 4H), 8.43 (d, $J = 4.8$ Hz, 4H), 9.53 (br, 2H) ppm; ¹³C NMR (100 MHz, DMSO-*d*₆): δ 49.8, 60.2, 122.7, 123.6, 125.4, 125.9, 127.4, 128.1, 128.9, 130.0, 133.6, 134.7, 137.1, 154.7 ppm; MS (ESI) m/z : 815 [M–2Cl[–]+H]²⁺; Anal. Calcd for C₅₄H₄₆Cl₂N₄O₄: C 73.21, H 5.23, N 6.32; found: C 72.92, H 5.18, N 5.98.

Acknowledgements

This work was supported by grants from the National NSF of China (Nos. 20602027 and 20702035) and the Outstanding Young

Scientist Award of Sichuan Province. We thank the Centre of Testing & Analysis, Sichuan University for NMR measurements.

Notes and references

- (a) D. A. Bender, *Amino Acid Metabolism*, 2nd edn, Wiley, New York, 1985; (b) G. Huether, *Amino Acid Availability and Brain Function in Health and Disease*, Springer, Heidelberg, 1988.
- (a) C. Schmuck, *Coord. Chem. Rev.*, 2006, **250**, 3053; (b) G. V. Oshovsky, D. N. Reinhoudt and W. Verboom, *Angew. Chem., Int. Ed.*, 2007, **46**, 2366.
- For selected examples, see: (a) T. Grawe, T. Schrader, P. Finocchiaro, G. Consiglio and S. Failla, *Org. Lett.*, 2001, **3**, 1597; (b) S.-Y. Liu, L. Fang, Y.-B. He, W.-H. Chan, K.-T. Yeung, Y.-K. Cheng and R.-H. Yang, *Org. Lett.*, 2005, **7**, 5825; (c) K.-S. Lee, T.-K. Kim, J. H. Lee, H.-J. Kim and J.-I. Hong, *Chem. Commun.*, 2008, 6173; (d) D. Leung, J. F. Folmer-Andersen, V. M. Lynch and E. V. Anslyn, *J. Am. Chem. Soc.*, 2008, **130**, 12318; (e) D.-L. Ma, W.-L. Wong, W.-H. Chung, F.-Y. Chan, P.-K. So, T.-S. Lai, Z.-Y. Zhou, Y.-C. Leung and K.-Y. Wong, *Angew. Chem., Int. Ed.*, 2008, **47**, 3735.
- For selected examples, see: (a) S.-G. Kim, K.-H. Kim, Y. K. Kim, S. K. Shin and K. H. Ahn, *J. Am. Chem. Soc.*, 2003, **125**, 13819; (b) A. Ragusa, S. Rossi, J. M. Hayes, M. Stein and J. D. Kilburn, *Chem.–Eur. J.*, 2005, **11**, 5674; (c) A. V. Yakovenko, V. I. Boyko, V. I. Kalchenko, L. Baldini, A. Casnati, F. Sansone and R. Ungaro, *J. Org. Chem.*, 2007, **72**, 3223; (d) Y. K. Kim, H. N. Lee, N. J. Singh, H. J. Choi, J. Y. Xue, K. S. Kim, J. Yoon and M. H. Hyun, *J. Org. Chem.*, 2008, **73**, 301.
- For reviews, see: (a) P. D. Beer, *Acc. Chem. Res.*, 1998, **31**, 71; (b) M. D. Best, S. L. Tobey and E. V. Anslyn, *Coord. Chem. Rev.*, 2003, **240**, 3; (c) J. M. Llinares, D. Powell and K. Bowman-James, *Coord. Chem. Rev.*, 2003, **240**, 57; (d) J. Yoon, S. K. Kim, N. J. Singh and K. S. Kim, *Chem. Soc. Rev.*, 2006, **35**, 355; (e) P. Blondeau, M. Segura, R. Pérez-Fernández and J. de Mendoza, *Chem. Soc. Rev.*, 2007, **36**, 198.
- (a) M. Boiocchi, M. Bonizzoni, L. Fabbri, G. Piovani and A. Taglietti, *Angew. Chem., Int. Ed.*, 2004, **43**, 3847; (b) C. Bazzicalupi, A. Bencini, A. Bianchi, L. Borsari, C. Giorgi and B. Valtancoli, *J. Org. Chem.*, 2005, **70**, 4257.
- (a) J. Raker and T. E. Glass, *J. Org. Chem.*, 2002, **67**, 6113; (b) C. Schmuck and M. Schwegmann, *J. Am. Chem. Soc.*, 2005, **127**, 3373.
- (a) P. P. Neelakandan, M. Hariharan and D. Ramaiah, *J. Am. Chem. Soc.*, 2006, **128**, 11334; (b) A. Schiller, R. A. Wessling and B. Singaram, *Angew. Chem., Int. Ed.*, 2007, **46**, 6457.
- (a) F. Sancenón, R. Martínez-Máñez, M. A. Miranda, M.-J. Seguí and J. Soto, *Angew. Chem., Int. Ed.*, 2003, **42**, 647; (b) C. Bazzicalupi, A. Bencini, A. Bianchi, A. Danesi, C. Giorgi, M. M. A. Lorente and B. Valtancoli, *New J. Chem.*, 2006, **30**, 959.
- (a) L. Fabbri, F. Foti and A. Taglietti, *Org. Lett.*, 2005, **7**, 2603; (b) A. Ojida, I. Takashima, T. Kohira, H. Nonaka and I. Hamachi, *J. Am. Chem. Soc.*, 2008, **130**, 12095.
- T. L. Amyes, S. T. Diver, J. P. Richard, F. M. Rivas and K. Toth, *J. Am. Chem. Soc.*, 2004, **126**, 4366.
- For selected examples after 2006, see: (a) N. J. Singh, E. J. Jun, K. Chellappan, D. Thangadurai, R. P. Chandran, I.-C. Hwang, J. Yoon and K. S. Kim, *Org. Lett.*, 2007, **9**, 485; (b) V. K. Khatri, M. Chahar, K. Pavani and P. S. Pandey, *J. Org. Chem.*, 2007, **72**, 10224; (c) P. P. Neelakandan and D. Ramaiah, *Angew. Chem., Int. Ed.*, 2008, **47**, 8407; (d) Q.-S. Lu, L. Dong, J. Zhang, J. Li, L. Jiang, Y. Huang, S. Qin, C.-W. Hu and X.-Q. Yu, *Org. Lett.*, 2009, **11**, 669.
- For reviews, see: (a) L. Pu, *Chem. Rev.*, 1998, **98**, 2405; (b) L. Pu, *Chem. Rev.*, 2004, **104**, 1687.
- For selected recent examples, see: (a) J. Zhao, T. M. Fyles and T. D. James, *Angew. Chem., Int. Ed.*, 2004, **43**, 3461; (b) Q. Wang, X. Chen, L. Tao, L. Wang, D. Xiao, X.-Q. Yu and L. Pu, *J. Org. Chem.*, 2007, **72**, 97; (c) Z.-B. Li, J. Lin, M. Sabat, M. Hyacinth and L. Pu, *J. Org. Chem.*, 2007, **72**, 4905; (d) H. Park, R. Nandhakumar, J. Hong, S. Ham, J. Chin and K. M. Kim, *Chem.–Eur. J.*, 2008, **14**, 9935.
- (a) J.-S. You, X.-Q. Yu, G.-L. Zhang, Q.-X. Xiang, J.-B. Lan and R.-G. Xie, *Chem. Commun.*, 2001, 1816; (b) Y. Yuan, G. Gao, Z.-L. Jiang, J.-S. You, Z.-Y. Zhou, D.-Q. Yuan and R.-G. Xie, *Tetrahedron*, 2002, **58**, 8993; (c) W. Chen, Y. Zhang, L. Zhu, J. Lan, R. Xie and J. You, *J. Am. Chem. Soc.*, 2007, **129**, 13879; (d) W.-H. Wang, P.-H. Xi, X.-Y. Su, J.-B. Lan, Z.-H. Mao, J.-S. You and R.-G. Xie, *Cryst. Growth Des.*,

- 2007, **7**, 741; (e) S. Zhang, S. Yang, J. Lan, Y. Tang, Y. Xue and J. You, *J. Am. Chem. Soc.*, 2009, **131**, 1689.
- 16 G. A. Hembury, V. V. Borovkov and Y. Inoue, *Chem. Rev.*, 2008, **108**, 1.
- 17 H. T. Stock and R. M. Kellogg, *J. Org. Chem.*, 1996, **61**, 3093.
- 18 F. Yang, S. Wei, C.-A. Chen, P. Xi, L. Yang, J. Lan, H.-M. Gau and J. You, *Chem.–Eur. J.*, 2008, **14**, 2223.
- 19 Y. Hamashima, D. Sawada, M. Kanai and M. Shibasaki, *J. Am. Chem. Soc.*, 1999, **121**, 2641.
- 20 CCDC 729190 contains the supplementary crystallographic data for this paper. These data can be obtained free of charge from The Cambridge Crystallographic Data Centre via www.ccdc.cam.ac.uk/data_request/cif.
- 21 Crystal data for (*R*)-**5**: C₃₄H₄₆Cl₂N₄O₄, *M* = 885.85, monoclinic, space group *C*2, *a* = 25.2548(3), *b* = 16.7371(9), *c* = 13.4129(10) Å, α = 90, β = 101.541(7), γ = 90°, *V* = 5554.9(6) Å³, *Z* = 4, *T* = 100(2) K, *D_c* = 1.059 g cm⁻³, *F*(000) = 1856, reflections collected = 14 647, independent reflections = 10 224 (*R*_{int} = 0.0308), Final *R* indices [*I* > 2σ(*I*)]: *R*₁ = 0.0621, *wR*₂ = 0.1277, *R* indices (all data): *R*₁ = 0.1068, *wR*₂ = 0.1347, GOF = 1.085.
- 22 (a) J. E. Miller, C. Grădinaru, B. R. Crane, A. J. Di Bilo, W. A. Wehbi, S. Un, J. R. Winkler and H. B. Gray, *J. Am. Chem. Soc.*, 2003, **125**, 14220; (b) G. M. Mackay, C. M. Forrest, N. Stoy, J. Christofides, M. Egerton, T. W. Stone and L. G. Darlington, *Eur. J. Neurol.*, 2006, **13**, 30.
- 23 (a) R. B. Rosse, B. L. Schwartz, S. Zlotolow, M. Bancy-Schwartz, A. C. Trinidad, T. D. Peace and S. I. Deutsch, *Clin. Neuropharmacol.*, 1992, **15**, 129; (b) B. L. Williamson, K. Klarskov, A. J. Tomlinsion, G. J. Gleich and S. Naylor, *Nat. Med.*, 1998, **4**, 983.
- 24 (a) Z. Bao, S. Sun, J. Li, X. Chen, S. Dong and H. Ma, *Angew. Chem., Int. Ed.*, 2006, **45**, 6723; (b) M. Hariharan, S. C. Karunakaran and D. Ramaiah, *Org. Lett.*, 2007, **9**, 417; (c) M. Fojta, S. Billová, L. Havran, H. Pivoňková, H. Černocká, P. Horáková and E. Paleček, *Anal. Chem.*, 2008, **80**, 4598.
- 25 (a) R. E. Galian, L. Pastor-Perez, M. A. Miranda and J. Perez-Prieto, *Chem.–Eur. J.*, 2005, **11**, 3443; (b) X. Wang and W. M. Nau, *J. Am. Chem. Soc.*, 2004, **126**, 808.
- 26 When excited at 369 nm, the Raman scattering peaks of water in the emission spectra of receptors (*R*)-**1**, (*R*)-**2**, (*R*)-**3** and (*R*)-**4** could be neglected. For some similar reports, see: (a) H. N. Lee, Z. Xu, S. K. Kim, K. M. K. Swamy, Y. Kim, S.-J. Kim and J. Yoon, *J. Am. Chem. Soc.*, 2007, **129**, 3828; (b) M. Yuan, Y. Li, J. Li, C. Li, X. Liu, J. Lv, J. Xu, H. Liu, S. Wang and D. Zhu, *Org. Lett.*, 2007, **9**, 2313. Also see 3*b*, 3*c* and 24*b*.
- 27 (a) H. A. Benesi and J. H. Hildebrand, *J. Am. Chem. Soc.*, 1949, **71**, 2703; (b) S. Fery-Forgues, M. T. Le Bris, J. P. Guette and B. Valeur, *J. Phys. Chem.*, 1988, **92**, 6233; (c) I. Schlachter, U. Höweler, W. Iwanek, M. Urbaniak and J. Mattay, *Tetrahedron*, 1999, **55**, 14931.
- 28 G. M. Scheldrick, *SHELX-97 and SHELXL-97, Program for Solution and Refinement of Crystal Structures*, University of Göttingen, Germany, 1997.
- 29 (a) H. Gilman, J. A. Beel, C. G. Brannen, M. W. Bullock, G. E. Dunn and L. S. Miller, *J. Am. Chem. Soc.*, 1949, **71**, 1499; (b) H. Gilman and A. H. Haubein, *J. Am. Chem. Soc.*, 1944, **66**, 1515.